No Impact of Functional Connectivity of the Motor System on the Resting Motor Threshold: A Replication Study

Melina Engelhardt[1,2]*, Darko Komnenić[3], Fabia Roth[1], Leona Kawelke[1], Carsten Finke[2,3,4] and Thomas Picht[1,2,5]

[1] *Charité – Universitätsmedizin Berlin, Department of Neurosurgery, Berlin, Germany,* [2] *Charité – Universitätsmedizin Berlin, Einstein Center for Neurosciences, Berlin, Germany,* [3] *Berlin School of Mind and Brain, Humboldt-Universität zu Berlin, Berlin, Germany,* [4] *Charité – Universitätsmedizin Berlin, Department of Neurology, Berlin, Germany,* [5] *Cluster of Excellence Matters of Activity, Image Space Material, Humboldt-Universität zu Berlin, Berlin, Germany*

The physiological mechanisms of corticospinal excitability and factors influencing its measurement with transcranial magnetic stimulation are still poorly understood. A recent study reported an impact of functional connectivity (FC) between the primary motor cortex (M1) and the dorsal premotor cortex (PMd) on the resting motor threshold (RMT) of the dominant hemisphere. We aimed to replicate these findings in a larger sample of 38 healthy right-handed subjects with data from both hemispheres. Resting-state FC was assessed between the M1 and five *a priori* defined motor-relevant regions on each hemisphere as well as interhemispherically between both primary motor cortices. Following the procedure by the original authors, we included age, cortical gray matter volume, and coil-to-cortex distance (CCD) as further predictors in the analysis. We report replication models for the dominant hemisphere as well as an extension to data from both hemispheres and support the results with Bayes factors. FC between the M1 and the PMd did not explain the variability in the RMT, and we obtained moderate evidence for the absence of this effect. In contrast, CCD could be confirmed as an important predictor with strong evidence. These findings contradict the previously proposed effect, thus questioning the notion of the PMd playing a major role in modifying corticospinal excitability.

Keywords: resting motor threshold, transcranial magnetic stimulation, functional connectivity, resting-state fMRI, variability

INTRODUCTION

The resting motor threshold (RMT) is a fundamental measurement in transcranial magnetic stimulation (TMS) studies. It is commonly used as an indicator of cortical excitability and as a basic dosing unit for TMS-based therapeutic interventions. These interventions have seen usage in multiple disciplines ranging from studies in motor cortical mapping, depression, language, and

---

Abbreviations: BF, Bayes factor; CCD, coil-to-cortex distance; CI, confidence interval; FA, fractional anisotropy; FC, functional connectivity; M1, primary motor cortex; PMd, dorsal premotor cortex; PMv, ventral premotor cortex; RMT, resting motor threshold; ROI, region-of-interest; rsfMRI, resting-state functional magnetic resonance imaging; SMA, supplementary motor area; S1, primary somatosensory cortex; TMS, transcranial magnetic stimulation.

vision [for an overview of different stimulation protocols, see Lefaucheur et al. (2014)]. Despite its prevalent use, the RMT's underlying physiological mechanisms and modulating factors are still poorly understood (Wassermann, 2002; Herbsman et al., 2009; Hübers et al., 2012). To assure an accurate RMT assessment, specifically when used as an outcome measurement to assess treatment effect, potential confounders need to be identified, and their influence minimized.

The RMT is defined as the smallest stimulation intensity to reliably elicit motor evoked potentials in a target muscle using TMS (Caramia et al., 1989; Rossini et al., 1994, 2015; Rothwell et al., 1999). It is used to capture the excitability of the stimulated cortical motor areas. Specifically, it reflects the transsynaptic activation of the corticospinal neurons as it can be modulated by changing the conductivity of the presynaptic sodium or calcium channels (Ziemann et al., 1996).

Several studies (Wassermann, 2002; Bhandari et al., 2016; Latorre et al., 2019) have shown a substantial variability in the RMT between and within healthy subjects. While the impact of methodological factors, such as the TMS equipment, use of neuronavigation software, and algorithms used to assess the RMT, is well established, the effects of structural and functional factors are still poorly understood (Herbsman et al., 2009; Hübers et al., 2012; Rosso et al., 2017). Recent studies have shown a positive correlation of the RMT with subject age after maturation of the white matter, a relationship potentially mediated by a reduction of cortical volume and an increase in coil-to-cortex distance (CCD; Bhandari et al., 2016; Rosso et al., 2017). Independent of age, CCD has been replicated as an important predictor of the RMT (Kozel et al., 2000; McConnell et al., 2001; Stokes et al., 2005). Furthermore, cortical thickness of the motor hand knob was positively correlated with the RMT in one study (List et al., 2013). Results are conflicting regarding the impact of white matter properties assessed using diffusion tensor imaging, e.g., fractional anisotropy (FA). Initial results (Klöppel et al., 2008) showing an inverse relationship between RMT and FA could not be replicated in subsequent studies (Herbsman et al., 2009; Hübers et al., 2012).

Rosso et al. (2017) were the first to study the impact of functional connectivity (FC) measured with resting-state functional magnetic resonance imaging (rsfMRI) on the RMT, thereby including a measure of functional integration of motor information. They predicted the RMTs of the dominant hemisphere with FC between the primary motor cortex (M1) and supplementary motor area (SMA), pre-SMA, dorsal premotor cortex (PMd), primary somatosensory cortex (S1), and the contralateral M1 using data of 21 participants. The impact of FC was then compared against known predictors, such as age and CCD, as well as other factors, such as FA and the cortical volume of these regions. The analysis showed a negative correlation between FC M1–PMd and RMT, which was confirmed in a multiple regression analysis including age, CCD, and the cortical volume of the dominant hemisphere as well. The authors, therefore, concluded that the cortical excitability of the M1 is critically impacted by integration of information from the PMd *via* cortico-cortical connections.

The aim of this study was to replicate these findings on the impact of FC M1–PMd in a larger sample and to assess their validity for the non-dominant hemisphere. We matched our sample in terms of age and gender distribution and followed the experimental design outlined by Rosso et al. (2017). We deviated from their paradigm only by using an atlas for delineation of the seed regions and focusing on the FC analysis, thus not investigating the impact of FA. Rosso et al. (2017) were contacted to inquire about details of the fMRI preprocessing and experimental setting, but were not included in any other way in this study. After this initial contact, we further included an exploratory analysis of the impact of the timing between the MRI and TMS procedures on our results.

MATERIALS AND METHODS

As the present study was a replication attempt, we followed the experimental and analysis procedures of Rosso et al. (2017) as closely as possible. The software and protocols used for acquisition of the MRI data were similar to those used in Rosso et al. (2017), and the analysis was identical. The remaining differences are specifically stated as such in the following methods. One deviation that became apparent only after contacting Rosso et al. (2017) was differences in the timing of the MRI and TMS procedures. While the MRI and TMS procedures were performed consecutively in the study by Rosso et al. (2017), only a subset of our sample received both measures on the same day. We tried to account for these differences by including an exploratory analysis of this subset.

Participants

Thirty-eight healthy, right-handed subjects (mean age $\pm$ SD: 37.5 ± 13.8 years, 21 females) participated in the study. Seven of these subjects (mean age $\pm$ SD: 41.9 ± 18.5 years, five females) received the MRI immediately before the TMS procedure. Handedness was assessed by the Edinburgh Handedness Inventory (Oldfield, 1971). Data were derived from two parallel studies (EA4/015/18, EA4/070/17) conducted at Charité. The inclusion criteria were (i) no history of neurological or psychiatric illness, (ii) age older than 18 years, (iii) no contraindications for TMS or MRI assessment, (iv) ability to provide written informed consent, and (v) right-handedness. All study procedures were approved by the local ethics committee, and the study was conducted in accordance with the Declaration of Helsinki. All subjects provided their written informed consent.

MRI
Image Acquisition
Magnetic resonance imaging (MRI) scans were performed on a Siemens 3-T Magnetom Trio MRI scanner (Siemens AG, Erlangen, Germany) with a 32-channel head coil. The MRI protocol took approximately 20 min and comprised a T1-weighted anatomical MPRAGE sequence (TR = 2,530 ms, TE = 4.94 ms, TI = 1,100 ms, flip angle = 7°, voxel size = 1 mm $\times$ 1 mm $\times$ 1 mm, 176 slices) and an rsfMRI sequence (TR = 2,000 ms, TE = 30 ms, flip angle = 78°, voxel

size = 3 mm × 3 mm × 3 mm, 238 volumes). For the rsfMRI sequence, subjects were instructed to close their eyes and let their thoughts flow freely.

rsfMRI FC

Analysis of the rsfMRI FC was performed using the SPM-based Toolbox CONN (version 18b; Whitfield-Gabrieli and Nieto-Castanon, 2012). The functional and structural images were pre-processed using CONN's default preprocessing pipeline (Nieto-Castanon, 2020). This includes the following steps: functional images were realigned to the first scan of the sequence and then slice-time corrected. Potential outlier scans with framewise displacement above 0.5 mm or global blood oxygen level dependent (BOLD) signal changes above 3 standard deviations (according to the "conservative" standard in CONN) were identified. Anatomical and functional images were then normalized into the Montreal Neurological Institute (MNI) space and segmented into the gray matter, white matter, and cerebrospinal fluid. Finally, functional data were smoothed using a Gaussian kernel of 8 mm full width half maximum. The default denoising pipeline as implemented in CONN (Nieto-Castanon, 2020) was used subsequently. The performed procedures consist of a regression to remove potentially confounding components from the white matter or cerebrospinal fluid, subject motion, and previously identified outlier scans to improve the signal-to-noise ratio. The data were then band-pass filtered to retain frequencies from 0.008 to 0.1 Hz.

Following preprocessing, region-of-interest (ROI)-to-ROI FC matrices were computed by selecting the corresponding option within the first-level analysis segment in the CONN toolbox. Each element of the connectivity matrices represents a Fisher's z-transformed bivariate correlation between a pair of ROI BOLD time series for one subject (Nieto-Castanon, 2020). Deviating from Rosso et al. (2017), the Human Motor Area Template (Mayka et al., 2006) was used to define the ROIs included in the analysis in the MNI space. This approach was chosen as it presents an objective, but time-efficient way to delineate ROIs in a larger number of subjects. Furthermore, we decided to use this specific atlas as it matches the regions included in the original article with the inclusion of one additional ROI in the ventral premotor cortex (PMv). The following ROI-to-ROI FC values were included in the analysis within each hemisphere: M1–S1, M1–SMA, M1–pre-SMA, M1–PMd, and M1–PMv. Additionally, interhemispheric FC was measured between the right M1 and the left M1 (M1–M1).

Cortical Gray Matter Volume

The cortical gray matter volume of each hemisphere was analyzed by FreeSurfer (version 7.1.0)[1] using the recon-all command. Briefly, this procedure includes motion correction, removal of non-brain tissue, Talairach transformation, segmentation of the gray and white matter structures, intensity normalization, and cortical parcelation (Fischl and Dale, 2000; Fischl, 2004; Reuter et al., 2012).

[1] http://surfer.nmr.mgh.harvard.edu/

Coil-to-Cortex Distance

For measurement of the CCD, individual structural MRIs were analyzed using itk-SNAP (version 3.8.0[2]; Yushkevich et al., 2006). The hand knob was localized for each hemisphere on the brain surface, and the shortest distance between the cortical surface of the hand knob and the surface of the scalp was assessed.

Neuronavigated TMS

Neuronavigated TMS (NTMS) was applied using a Nexstim NBS5 stimulator (Nexstim, Helsinki, Finland) with a figure-of-eight coil (outer diameter: 70 mm). Each subject's structural MRI was used as a subject-specific navigational dataset. Motor evoked potentials were recorded in a belly tendon fashion from the first dorsal interosseous muscles of both hands with disposable Ag/AgCl surface electrodes (Neuroline 700; Ambu, Ballerup, Denmark). The ground electrode was attached to the left palmar wrist. Subjects were instructed to sit comfortably in the chair and relax their hand muscles. Muscle activity was monitored to assure relaxation of the muscle, with a maximum tolerated baseline activity of 10 μV. The stimulation site, electric field direction and angulation consistently eliciting the largest motor evoked potentials in the target muscle was defined as the hotspot for stimulation and stored in the system. For this point, the RMT was defined according to the Rossini–Rothwell method (Rossini et al., 1994; Rothwell et al., 1999) as the lowest stimulation intensity to elicit motor evoked potentials larger than 50 μV in at least five out of 10 trials. The RMT was recorded as a percentage of the maximum stimulator output.

Statistical Analysis

Statistical analyses were conducted in RStudio (version 1.3.1073)[3]. Analysis was divided to first replicate results for the dominant hemisphere only (replication analysis) and second to extend these findings to the whole dataset with data from both hemispheres (extended analysis). Finally, we tested the multiple regression model for the dominant hemisphere and linear mixed model for both hemispheres for the subset of participants ($n = 7$) who received the TMS procedure directly after the MRI. These last analyses should be interpreted with caution due to the small sample size of this subset of the data. Nevertheless, we decided to include these illustrative analyses to give some idea about the impact of the timing between MRI and TMS as procedural deviation between both studies.

To assess the relationship between RMT and all included predictors alone, we replicated the correlation analyses of Rosso et al. (2017) for the data of the dominant hemisphere. Correlation coefficients, 95% confidence intervals (CIs), and p-values are stated in **Table 1**. For the extended analysis, these relationships were quantified by linear mixed models with subjects as random intercepts. Estimates for fixed effects with 95% CIs are presented together with t- and p-values approximated with the Satterthwaite's method (**Table 2**).

In the replication analysis, we calculated the multiple linear regression model of Rosso et al. (2017) with the RMT as

[2] www.itksnap.org
[3] http://www.rstudio.com/

TABLE 1 | Correlation coefficients for the dominant hemisphere.

Dependent variable	Independent variable	Correlation coefficient[a]	*t*-value	*p*-value	BF$_{10}$
RMT	CCD	0.626 (0.383, 0.788)	4.813	<0.001*	784.65
	Age	0.066 (−0.260, 0.377)	0.394	0.696	0.39
	Gray matter volume	−0.187 (−0.478, 0.141)	−1.144	0.260	0.63
	FC M1–M1	−0.130 (−0.432, 0.198)	−0.787	0.436	0.47
	FC M1–S1	0.043 (−0.281, 0.358)	0.257	0.799	0.37
	FC M1–SMA	−0.156 (−0.453, 0.172)	−0.950	0.348	0.53
	FC M1–pre-SMA	0.019 (−0.303, 0.336)	0.112	0.911	0.36
	FC M1–PMd	0.041 (−0.282, 0.356)	0.249	0.805	0.37
	FC M1–PMv	0.104 (−0.223, 0.410)	0.627	0.535	0.43
Age	Gray matter volume	−0.557 (−0.744, −0.289)	−4.027	<0.001*	114.69

[a]*Presented with 95% confidence intervals.*
**p-values below 0.05 were considered significant.*

TABLE 2 | Multiple regression model for the dominant hemisphere.

Dependent variable	Independent variable	Estimate[a]	*t*-value	*p*-value	Partial R^{2a}	BF$_{10}$
RMT	CCD	1.531 (0.864, 2.198)	4.669	<0.001*	0.398 (0.173, 0.620)	2.48 × 10^3
	Age	−0.071 (−0.225, 0.083)	−0.935	0.356	0.003 (0.000, 0.153)	0.27
	Gray matter volume	−0.029 (−0.087, 0.030)	−0.935	0.328	0.029 (0.000, 0.227)	0.28
	FC M1–PMd	−1.529 (−12.116, 9.057)	−0.294	0.771	0.026 (0.000, 0.220)	0.17

[a]*Presented with 95% confidence intervals.*
**p-values below 0.05 were considered significant.*

dependent variable and age, the CCD, the cortical volume of the hemisphere, and FC M1–PMd as independent variables (**Table 3**). Estimates for regression coefficients with 95% CIs are given together with *t*- and *p*-values. Additionally, we computed the variance explained by the model R^2 as well as partial R^2 for each predictor with their respective 95% CIs. In the extension analysis, we calculated a linear mixed model with the RMT as dependent variable and age, the CCD, the cortical gray matter volume of the hemisphere, hemisphere (0 = dominant, 1 = non-dominant), and FC M1–PMd as fixed effects (**Table 4**). Subjects were included as random effect. Estimates for fixed effects with 95% CIs are given together with *t*- and *p*-values approximated with the Satterthwaite's method. Furthermore, R^2 (Model) and partial R^2 for each fixed effect with their respective 95% CIs were computed.

To assure the interpretability of the results of regression and mixed models, we calculated variance inflation factors as a measure of collinearity between predictors in each model. A variance inflation factor <5 suggests no collinearity between predictors. All models met this criterion. As in the original study, *p*-values ≤ 0.05 were considered significant.

While using these analyses with null hypothesis significance testing allows comparison with Rosso et al. (2017), it does not allow for rejection of the alternative hypothesis (Dienes, 2011, 2014). However, judgment of evidence for or against the null hypothesis is crucial to decide whether a replication was successful. To quantify this evidence, we calculated Bayes factors (BF$_{10}$) expressing evidence for the alternative hypothesis relative to the null hypothesis given the data. Thus, a BF > 1 provides anecdotal evidence for the alternative hypothesis (that is, the

variable in question influences the RMT), a BF > 3 provides moderate evidence, and a BF > 10 provides strong evidence. Conversely, a BF < 1 provides anecdotal evidence for the null hypothesis (that is, the variable in question does not influence the RMT), a BF < 0.33 provides moderate evidence, and a BF < 0.1 provides strong evidence (Jeffreys, 1961; Lee and Wagenmakers, 2014). BFs for a specific fixed effect were assessed by comparing the full model to the model without the factor of interest using the bayestestR package in R (Makowski et al., 2019). BFs for correlation coefficients were calculated using the BayesFactor package in R (Morey and Rouder, 2015).

RESULTS

Replication Analysis

All study procedures were tolerated well and without side effects. The RMT in the dominant hemisphere had a mean of 34.5% (standard deviation 5.9%, range 25–49%). The range of 24% was comparable to Rosso et al. (2017). The RMT was positively correlated with the CCD ($r = 0.626$, $p < 0.001$; **Figure 1A**). Aligning with Rosso et al. (2017), no correlation was observed between the RMT and the participants' age ($r = 0.066$, $p = 0.696$; **Figure 1B**), but the cortical gray matter volume and age ($r = −0.557$, $p < 0.001$). However, no meaningful correlation was found between the RMT and the cortical gray matter volume of the dominant hemisphere ($r = −0.187$, $p = 0.260$; **Figure 1C**) or FC M1–PMd ($r = 0.041$, $p = 0.805$; **Figure 1D**). There was no association between RMT and FC between any other pair of regions (**Table 1**).

TABLE 3 | Linear mixed models with single variables using data from both hemispheres.

Dependent variable	Independent variable	Estimate[a]	t-value[b]	p-value[b]	BF_{10}
RMT	CCD	1.448 (0.912, 1.976)	5.452	0.001*	1.59×10^4
	Age	0.026 (−0.111, 0.162)	0.378	0.708	0.12
	Gray matter volume	−0.022 (−0.080, 0.037)	−0.771	0.445	0.15
	FC M1–M1	−4.039 (−11.157, 3.079)	−1.141	0.261	0.22
	FC M1–S1	2.014 (−1.469, 5.491)	1.152	0.254	0.22
	FC M1–SMA	1.910 (−3.727, 7.368)	0.699	0.487	0.15
	FC M1–pre-SMA	−0.043 (−6.421, 6.329)	−0.013	0.989	0.12
	FC M1–PMd	−0.047 (−5.445, 5.256)	−0.017	0.986	0.12
	FC M1–PMv	−0.429 (−6.762, 6.041)	−0.137	0.891	0.12
	Hemisphere	−1.079 (−2.358, 0.201)	−1.695	0.098	0.46
Gray matter volume	Age	−1.2847 (−1.907, −0.663)	−4.153	<0.001*	140.31

[a] Presented with 95% confidence intervals.
[b] t- and p-values were approximated with the Satterthwaite's method.
*p-values below 0.05 were considered significant.

TABLE 4 | Combined linear mixed model for both hemispheres.

Dependent variable	Independent variable	Estimate[a]	t-value[b]	p-value[b]	Partial R^{2a}	BF_{10}
RMT	CCD	1.468 (0.928, 1.999)	5.508	<0.001*	0.425 (0.271, 0.574)	1.8×10^4
	Age	0.034 (0.000, 0.156)	−1.080	0.287	−0.070 (−0.198, 0.061)	0.2
	Gray matter volume	0.021 (0.000, 0.131)	−0.823	0.415	−0.022 (−0.076, 0.032)	0.16
	FC M1–PMd	0.810 (−4.087, 5.710)	0.329	0.743	0.001 (0.000, 0.074)	0.12
	Hemisphere	−0.994 (−2.214, 0.227)	−1.638	0.110	0.016 (0.000, 0.118)	0.42

[a] Presented with 95% confidence intervals.
[b] t- and p-values were approximated with the Satterthwaite's method.
*p-values below 0.05 were considered significant.

The multiple regression model explained 42% [R^2; 95% CI (23.4, 65.5%); **Figure 1E**] of the variance in the RMT. In contrast to Rosso et al. (2017), only the CCD was predictive of the RMT in this model, whereas FC M1–PMd and the gray matter volume did not show an effect. Finally, age was not associated with the RMT. We obtained strong evidence for the impact of the CCD on the RMT ($BF_{10} = 2.48 \times 10^3$). In contrast, the BFs of the effect of FC M1–PMd ($BF_{10} = 0.17$), gray matter volume ($BF_{10} = 0.28$), and age ($BF_{10} = 0.27$) moderately favored the null hypothesis. Detailed results can be found in **Table 3**.
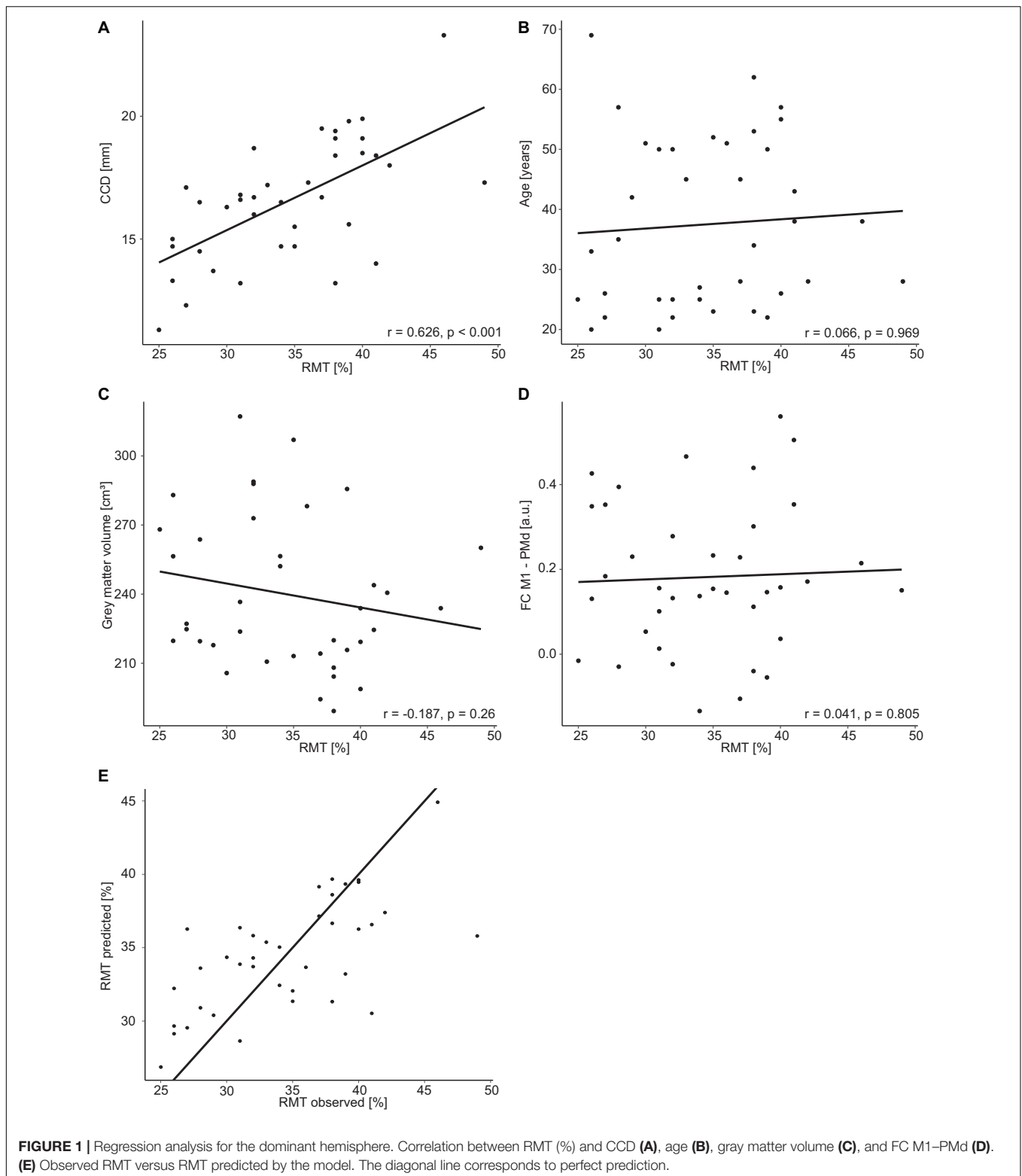
Extended Analysis

The mean RMT for both hemispheres was 34.0% (standard deviation 6.1%, range 23–51%). Comparable to the results for the dominant hemisphere, the RMT was positively associated with the CCD (estimate: 1.448, $p < 0.001$; **Figure 2A**). No association was found with participants' age (estimate: 0.026, $p = 0.708$; **Figure 2B**), cortical gray matter volume (estimate: −0.022, $p = 0.445$; **Figure 2C**), and FC M1–PMd (estimate: −0.047, $p = 0.986$; **Figure 2D**). Furthermore, the hemisphere stimulated did not impact the RMT (estimate: −1.079, $p = 0.098$; **Figure 2E**). Again, no association between RMT and FC between any other pair of regions was observed (**Table 2**).

The linear mixed model including age, CCD, cortical gray matter volume, and FC M1–PMd explained 44.4% [R^2; 95% CI (31.3, 60.2%); **Figure 2F**] of the variance in the RMT. Similar to

the multiple regression analysis, the CCD was the only significant predictor of the RMT. No association was found between RMT and FC M1–PMd, age, cortical gray matter volume, or hemisphere. There was strong evidence for the effect of the CCD on the RMT ($BF_{10} = 1.8 \times 10^4$). In contrast, there were moderate evidence for the null hypothesis when looking at FC M1–PMd ($BF_{10} = 0.12$), age ($BF_{10} = 0.2$), and cortical gray matter volume ($BF_{10} = 0.16$) and anecdotal evidence for the null hypothesis when looking at hemisphere ($BF_{10} = 0.42$). Detailed results can be found in **Table 4**.

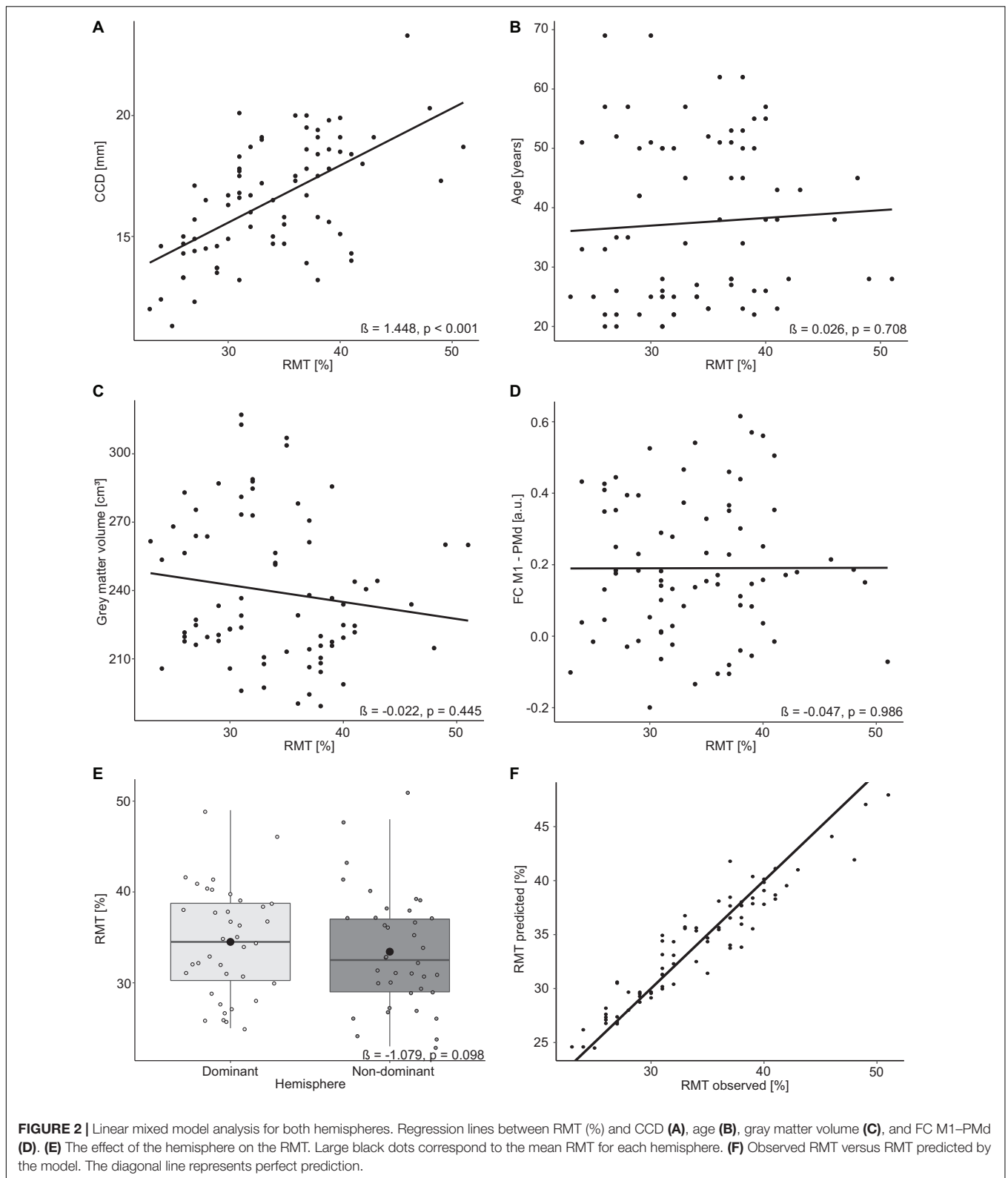### Analysis of Subgroup With Successive MRI and TMS

Finally, we repeated these analyses in the subgroup of participants who received their MRI directly before the TMS. The mean RMT for the dominant hemisphere in this subset was 33.1% (standard deviation 5.4%, range 26–39%). The multiple regression model for the dominant hemisphere explained 91% [R^2; 95% CI (71.2, 99.8%)] of the variance in the RMT. None of the tested parameters reached significance for predicting the RMT (**Table 5**), which can most likely be explained by the small sample size. We still obtained strong evidence for the impact of CCD ($BF_{10} = 93.37$) and age ($BF_{10} = 142.68$) on the RMT. In contrast, the BFs of the effect of FC M1–PMd ($BF_{10} = 0.39$) and gray matter volume ($BF_{10} = 0.70$) gave anecdotal evidence for the null hypothesis. Importantly, the relationship between RMT and

FIGURE 1 | Regression analysis for the dominant hemisphere. Correlation between RMT (%) and CCD **(A)**, age **(B)**, gray matter volume **(C)**, and FC M1–PMd **(D)**. **(E)** Observed RMT versus RMT predicted by the model. The diagonal line corresponds to perfect prediction.

FC M1–PMd estimated here was also positive and thus in the opposite direction compared with Rosso et al. (2017).

The mean RMT for both hemispheres in this subset was 33.1% (standard deviation 5.2%, range 26–41%). The linear

mixed model including data from both hemispheres explained 84.4% [R^2; 95% CI (70.1, 95.1%)] of the variance in the RMT. CCD and age were significant predictors of the RMT. No association was found between RMT and FC M1–PMd,

FIGURE 2 | Linear mixed model analysis for both hemispheres. Regression lines between RMT (%) and CCD **(A)**, age **(B)**, gray matter volume **(C)**, and FC M1–PMd **(D)**. **(E)** The effect of the hemisphere on the RMT. Large black dots correspond to the mean RMT for each hemisphere. **(F)** Observed RMT versus RMT predicted by the model. The diagonal line represents perfect prediction.

cortical gray matter volume, or hemisphere. There were strong evidence for the effect of CCD ($BF_{10} = 62.07$) and age ($BF_{10} = 193.89$) on the RMT and anecdotal evidence for

cortical gray matter volume ($BF_{10} = 1.13$). In contrast, there was moderate evidence for the null hypothesis when looking at FC M1–PMd ($BF_{10} = 0.28$) and hemisphere ($BF_{10} = 0.30$).

TABLE 5 | Multiple regression model for the subgroup and dominant hemisphere.

Dependent variable	Independent variable	Estimate[a]	t-value	p-value	Partial R^{2a}	BF$_{10}$
RMT	CCD	1.661 (−0.903, 4.226)	2.787	0.108	0.795 (0.236, 0.994)	93.37
	Age	−0.303 (−0.741, 0.134)	−2.983	0.096	0.816 (0.304, 0.995)	142.68
	Gray matter volume	−0.033 (−0.263, 0.196)	−0.623	0.597	0.163 (0.000, 0.964)	0.70
	FC M1–PMd	1.078 (−36.188, 38.345)	0.124	0.912	0.008 (0.000, 0.951)	0.39

[a] Presented with 95% confidence intervals.

TABLE 6 | Combined linear mixed model for the subgroup and both hemispheres.

Dependent variable	Independent variable	Estimate[a]	t-value[b]	p-value[b]	Partial R^{2a}	BF$_{10}$
RMT	CCD	1.486 (0.770, 2.257)	4.508	0.002	0.673 (0.360, 0.888)	62.07
	Age	−0.327 (−0.481, −0.189)	−4.967	<0.001*	0.714 (0.430, 0.902)	193.89
	Gray matter volume	−0.061 (−0.127, 0.013)	−2.015	0.087	0.292 (0.006, 0.715)	1.13
	FC M1–PMd	1.863 (−9.163, 13.348)	0.358	0.725	0.013 (0.000, 0.438)	0.28
	Hemisphere	−0.815 (−4.207, 2.610)	−0.505	0.624	0.025 (0.000, 0.462)	0.30

[a] Presented with 95% confidence intervals.
[b] t- and p-values were approximated with the Satterthwaite's method.
*p-values below 0.05 were considered significant.

Again, the estimated relationship between RMT and FC M1–PMd was positive and thus in the opposite direction compared with Rosso et al. (2017). Detailed results can be found in **Table 6**.

DISCUSSION

The present study aimed to replicate findings by Rosso et al. (2017) on the impact of rsfMRI FC on the RMT. Specifically, Rosso et al. (2017) proposed an influence of FC between the M1 and the PMd of the dominant hemisphere while accounting for known predictors, such as CCD, cortical gray matter volume, and age. In contrast to Rosso et al. (2017), we did not observe an influence of FC between any of the investigated motor regions on the RMT in either the dominant hemisphere or when taking into account data from both hemispheres. The absence of this effect was supported by BFs providing moderate evidence for the null hypothesis. The only significant predictor of the RMT was the CCD, whereas age, cortical gray matter volume, and hemisphere had no shown impact on the RMT. Notably, our models only explained a maximum of 44% of variance compared with 75% in the study by Rosso et al. (2017) using the same predictors.

The positive association between the CCD and the RMT due to the exponential decrease of the magnetic field with increasing distance from the coil is well established (Kozel et al., 2000; McConnell et al., 2001; Stokes et al., 2005). Consequently, any factor contributing to an increased distance, such as anatomical variability or brain atrophy, reduces the magnetic field reaching the cortical target areas. To elicit motor evoked potentials comparable in size, the stimulation intensity needs to be increased, leading to a higher RMT in these subjects (McConnell et al., 2001). It has, therefore, been suggested to measure the RMT in units of the electric field induced at the cortical level rather than the percentage of the stimulator output

as this should be less susceptible to the confounding impact of the CCD (Julkunen et al., 2012).

Contrary to our expectations, we were not able to observe an effect of age on the RMT in the present sample. Others found an increased RMT with age, with aging-related brain atrophy, leading to a larger CCD, being the main hypothesized underlying cause (Bhandari et al., 2016; Rosso et al., 2017). However, other studies have–similar to our findings–reported the absence of an age effect in their samples (Kozel et al., 2000; Wassermann, 2002). Similar to age, the cortical gray matter volume was also not predictive of the RMT in our sample. Nevertheless, age and cortical gray matter volume were negatively associated, hinting to the presence of age-related brain atrophy also in our sample.

Rosso et al. (2017) were the first to report an effect of FC between the M1 and the PMd on the RMT. They explained this effect by the known connectivity between both regions and potential facilitatory processes upon stimulation. The present study does not support these conclusions. However, this does not necessarily mean that FC does not impact the RMT at all, but rather that such an effect could not be captured using the present methodology. Recent studies (Zrenner et al., 2018; Desideri et al., 2019; Schaworonkow et al., 2019) have shown the state dependency of TMS-induced effects by investigating the size of motor evoked potentials during different phases of the mu-rhythm observed in human electroencephalography. They showed that the stimuli applied to the negative peak of the oscillation cause larger motor evoked potentials than those to the positive peak, thus describing a state of high or low excitability, respectively. While FC using rsfMRI can only be captured at timescales of several seconds (Babiloni et al., 2009; Yaesoubi et al., 2017), a similar state-dependency phenomenon might theoretically be observable using this measure. In support of this idea, Tagliazucchi et al. (2012) have related fluctuating FC with spectral power of different oscillation frequencies in electroencephalography, thus underpinning the

neurophysiological origin of FC states. Neither the original study (Rosso et al., 2017) nor this replication attempt would have been able to address this state-dependency hypothesis as MRI and TMS were not performed at the same time.

In support of our results, the present study was conducted in a sample almost twice as large as that of Rosso et al. (2017), with additional data from the non-dominant hemisphere. The sample was comparable in terms of participants' age and gender distribution as well as the range of recorded RMTs. We replicated the statistical analyses of Rosso et al. (2017) while including BFs as a measure to quantify evidence for the respective hypothesis. This is crucial for the current study as it enables us to make assumptions about the null hypothesis (Jeffreys, 1961; Dienes, 2011, 2014; Lee and Wagenmakers, 2014), thus giving evidence for the absence of an effect of FC on the RMT. All together, we followed the original protocol as closely as possible with some minor deviations, whose potential impacts on our results will be discussed in the following section.

(i) Differences in equipment. Both studies were conducted using a 3 T MRI scanner (Siemens AG, Erlangen, Germany) with a 32-channel head coil with almost identical scanning sequences. The rsfMRI sequence in the present study had a slightly shorter TR and larger number of volumes. Similarly, TMS systems differed between both studies (NBS5, Nexstim: maximal output 1.42 Tesla; Magstim 200^2, Magstim: maximal output 2.2 Tesla). However, both systems used a neuronavigation software to keep the coil positioning stable and determined the RMT manually (Rossini–Rothwell method; Rossini et al., 1994; Rothwell et al., 1999). While this impacted the absolute values of the RMT (13.5% higher average RMT in the original study compared with this study), the range of the RMTs relative to the absolute RMTs was comparable in both studies.

(ii) Timing of MRI and TMS. In the study by Rosso et al. (2017), participants received their TMS measurement directly after the MRI scan. In contrast, in the present study, the time between both measurements varied, with only seven subjects receiving them directly after another. To address this difference, we included an exploratory analysis for the subgroup of subjects who received the MRI directly before the TMS. It should be noted that this analysis can only give a rough estimate of any potential effect due to the small sample size in this subgroup. There was also no effect of FC on the RMT in this analysis. Most rsfMRI networks are fairly reproducible over time (Chou et al., 2012), thus reducing the impact of the time interval between both measurements. On the other hand, varying FC states can be observed even during the short scanning period (Hutchison et al., 2013; Allen et al., 2014; Preti et al., 2017; Battaglia et al., 2020), and this is further altered by execution of a task, such as subject's movement from MRI to TMS (Gonzalez-Castillo and Bandettini, 2018). Thus, also on a theoretical level, these factors again seem unlikely to explain deviating results.

(iii) Delineation of ROIs. Rosso et al. (2017) used subject-specific ROIs drawn on subjects' FA maps, whereas the present study used an atlas. Both approaches lead to comparable ROIs in terms of size and location, with the exception of an additional ROI for the PMv in the atlas used in this study (Mayka et al., 2006). Furthermore, Marrelec and Fransson (2011) show that the mean FC values are not impacted by the choice of the ROI delineation method, specifically when resulting differences in ROIs are small.

In conclusion, the present study does not support the concept of FC between the M1 and the PMd influencing the excitability of the corticospinal tract. The distance between the coil and the cortex remains the most important factor in explaining the variability in the RMTs, whereas other factors, such as age, gray matter volume, or hemisphere, seem to be less important. Consequently, results of the present study contradict the hypothesis of the RMT reflecting the variability of both anatomical and functional features of the motor system as proposed by Rosso et al. (2017). Growing evidence (Kozel et al., 2000; McConnell et al., 2001) highlights the impact of the CCD and the potential impact of other anatomical factors, such as microstructural properties of the corticospinal tract (Klöppel et al., 2008). In contrast, more research is needed to investigate the role of functional factors, such as state dependency of excitability, wakefulness, or the influence of medication. While anatomical factors should remain stable within the same individual over a short period and are thus more likely to explain interindividual differences in the RMTs, functional factors might be a promising target to explain the intraindividual variability of RMT measurements.

DATA AVAILABILITY STATEMENT

The datasets presented in this article are not readily available because no consent was obtained from subjects to publicly share their pseudonymized data or to anonymize the data. Requests to access the datasets should be directed to the corresponding author.

ETHICS STATEMENT

The studies involving human participants were reviewed and approved by the Ethics Committee of Charité – Universitätsmedizin Berlin. The patients/participants provided their written informed consent to participate in this study.

AUTHOR CONTRIBUTIONS

ME, CF, and TP designed the study. ME, FR, and LK collected the data. ME and DK processed the MRI data. ME performed the statistical analysis. ME and TP drafted the manuscript. ME, DK, FR, LK, CF, and TP provided critical revision.

REFERENCES

Allen, E. A., Damaraju, E., Plis, S. M., Erhardt, E. B., Eichele, T., and Calhoun, V. D. (2014). Tracking whole-brain connectivity dynamics in the resting state. *Cerebral Cortex* 24, 663–676. doi: 10.1093/cercor/bhs352

Babiloni, C., Pizzella, V., Del Gratta, C., Ferretti, A., and Romani, G. L. (2009). Chapter 5 Fundamentals of electroencefalography, magnetoencephalography, and functional magnetic resonance imaging. *Int. Rev. Neurobiol.* 86, 67–80. doi: 10.1016/S0074-7742(09)86005-4

Battaglia, D., Boudou, T., Hansen, E. C. A., Lombardo, D., Chettouf, S., Daffertshofer, A., et al. (2020). Dynamic functional connectivity between order and randomness and its evolution across the human adult lifespan. *NeuroImage* 222:117156. doi: 10.1016/j.neuroimage.2020.117156

Bhandari, A., Radhu, N., Farzan, F., Mulsant, B. H., Rajji, T. K., Daskalakis, Z. J., et al. (2016). A meta-analysis of the effects of aging on motor cortex neurophysiology assessed by transcranial magnetic stimulation. *Clin. Neurophysiol.* 127, 2834–2845. doi: 10.1016/j.clinph.2016.05.363

Caramia, M. D., Pardal, A. M., Zarola, F., and Rossini, P. M. (1989). Electric vs magnetic trans-cranial stimulation of the brain in healthy humans: a comparative study of central motor tracts 'conductivity' and 'excitability.'. *Brain Res.* 479, 98–104. doi: 10.1016/0006-8993(89)91339-5

Chou, Y.-H., Panych, L. P., Dickey, C. C., Petrella, J. R., and Chen, N.-K. (2012). Investigation of long-term reproducibility of intrinsic connectivity network mapping: a resting-state fmri study. *AJNR Am. J. Neuroradiol.* 33, 833–838. doi: 10.3174/ajnr.A2894

Desideri, D., Zrenner, C., Ziemann, U., and Belardinelli, P. (2019). Phase of sensorimotor µ-oscillation modulates cortical responses to transcranial magnetic stimulation of the human motor cortex. *J. Physiol.* 597, 5671–5686. doi: 10.1113/JP278638

Dienes, Z. (2011). Bayesian versus orthodox statistics: which side are you on? *Perspect. Psychol. Sci.* 6, 274–290. doi: 10.1177/1745691611406920

Dienes, Z. (2014). Using bayes to get the most out of non-significant results. *Front. Psychol.* 5:781. doi: 10.3389/fpsyg.2014.00781

Engelhardt, M., Darko, K., Fabia, R., Leona, K., Carsten, F., and Thomas, P. (2020). No impact of functional connectivity of the motor system on the resting motor threshold: a replication study. *BioRxiv [preprint]* doi: 10.1101/2020.10.26.354886

Fischl, B. (2004). Automatically parcellating the human cerebral cortex. *Cerebral Cortex* 14, 11–22. doi: 10.1093/cercor/bhg087

Fischl, B., and Dale, A. M. (2000). Measuring the thickness of the human cerebral cortex from magnetic resonance images. *Proc. Natl. Acad. Sci. U.S.A.* 97, 11050–11055. doi: 10.1073/pnas.200033797

Gonzalez-Castillo, J., and Bandettini, P. A. (2018). Task-Based dynamic functional connectivity: recent findings and open questions. *NeuroImage* 180, 526–533. doi: 10.1016/j.neuroimage.2017.08.006

Herbsman, T., Forster, L., Molnar, C., Dougherty, R., Christie, D., Koola, J., et al. (2009). Motor threshold in transcranial magnetic stimulation: the impact of white matter fiber orientation and skull-to-cortex distance. *Hum. Brain Mapp.* 30, 2044–2055. doi: 10.1002/hbm.20649

Hübers, A., Klein, J. C., Kang, J. S., Hilker, R., and Ziemann, U. (2012). The relationship between TMS measures of functional properties and DTI measures of microstructure of the corticospinal tract. *Brain Stimulat.* 5, 297–304. doi: 10.1016/j.brs.2011.03.008

Hutchison, R. M., Womelsdorf, T., Allen, E. A., Bandettini, P. A., Calhoun, V. D., Corbetta, M., et al. (2013). Dynamic functional connectivity: promise, issues, and interpretations. *NeuroImage* 80, 360–378. doi: 10.1016/j.neuroimage.2013.05.079

Jeffreys, H. (1961). *Theory of Probability*, Edn. 3 Edn. Oxford: Oxford University Press.

Julkunen, P., Säisänen, L., Danner, N., Awiszus, F., and Könönen, M. (2012). Within-Subject effect of coil-to-cortex distance on cortical electric field threshold and motor evoked potentials in transcranial magnetic stimulation. *J. Neurosci. Methods* 206, 158–164. doi: 10.1016/j.jneumeth.2012.02.020

Klöppel, S., Bäumer, T., Kroeger, J., Koch, M. A., Büchel, C., Münchau, A., et al. (2008). The cortical motor threshold reflects microstructural properties of cerebral white matter. *NeuroImage* 40, 1782–1791. doi: 10.1016/j.neuroimage.2008.01.019

Kozel, F. A., Nahas, Z., DeBrux, C., Molloy, M., Lorberbaum, J. P., Bohning, D., et al. (2000). How coil-cortex distance relates to age, motor threshold, and antidepressant response to repetitive transcranial magnetic stimulation. *J. Neuropsych. Clin. Neurosci.* 12, 376–384. doi: 10.1176/jnp.12.3.376

Latorre, A., Rocchi, L., Berardelli, A., Bhatia, K. P., and Rothwell, J. C. (2019). The interindividual variability of transcranial magnetic stimulation effects: implications for diagnostic use in movement disorders. *Mov. Disord.* 34, 936–949. doi: 10.1002/mds.27736

Lee, M. D., and Wagenmakers, E.-J. (2014). *Bayesian Cognitive Modeling: A Practical Course*. Cambridge: Cambridge university press.

Lefaucheur, J.-P., André-obadia, N., Antal, A., Ayache, S. S., Baeken, C., Benninger, D. H., et al. (2014). Clinical neurophysiology evidence-based guidelines on the therapeutic use of repetitive transcranial magnetic stimulation (rTMS). *Clin. Neurophysiol.* 125, 2150–2206. doi: 10.1016/j.clinph.2014.05.021

List, J., Kübke, J. C., Lindenberg, R., Külzow, N., Kerti, L., Witte, V., et al. (2013). Relationship between excitability, plasticity and thickness of the motor cortex in older adults. *NeuroImage* 83, 809–816. doi: 10.1016/j.neuroimage.2013.07.033

Makowski, D., Ben-Shachar, M., and Lüdecke, D. (2019). BayestestR: describing effects and their uncertainty, existence and significance within the bayesian framework. *J. Open Source Softw.* 4:1541. doi: 10.21105/joss.01541

Marrelec, G., and Fransson, P. (2011). Assessing the influence of different ROI selection strategies on functional connectivity analyses of FMRI data acquired during steady-state conditions. *PLoS One* 6:e14788. doi: 10.1371/journal.pone.0014788

Mayka, M. A., Corcos, D. M., Leurgans, S. E., and Vaillancourt, D. E. (2006). Three-dimensional locations and boundaries of motor and premotor cortices as defined by functional brain imaging: a meta-analysis. *NeuroImage* 31, 1453–1474. doi: 10.1016/j.neuroimage.2006.02.004

McConnell, K. A., Nahas, Z., Shastri, A., Lorberbaum, J. P., Kozel, F. A., Bohning, D. E., et al. (2001). The transcranial magnetic stimulation motor threshold depends on the distance from coil to underlying cortex: a replication in healthy

adults comparing two methods of assessing the distance to cortex. *Biol. Psych.* 49, 454–459. doi: 10.1016/S0006-3223(00)01039-8

Morey, R., and Rouder, J. N. (2015). *BayesFactor: Computation of Bayes Factors for Common Designs*. Available online at: https://cran.r-project.org/web/packages/BayesFactor/index.html (accessed October 13, 2020).

Nieto-Castanon, A. (2020). Handbook of Functional Connectivity Magnetic Resonance Imaging Methods in CONN. Hilbert Press.

Oldfield, R. C. (1971). The assessment and analysis of handedness: the edinburgh inventory. *Neuropsychologia* 9, 97–113. doi: 10.1016/0028-3932(71)90067-4

Preti, M. G., Bolton, T. A. W., and Van De Ville, D. (2017). The dynamic functional connectome: state-of-the-art and perspectives. *NeuroImage* 160, 41–54. doi: 10.1016/j.neuroimage.2016.12.061

Reuter, M., Schmansky, N. J., Rosas, H. D., and Fischl, B. (2012). Within-Subject template estimation for unbiased longitudinal image analysis. *NeuroImage* 61, 1402–1418. doi: 10.1016/j.neuroimage.2012.02.084

Rossini, P. M., Barker, A. T., and Berardelli, A. (1994). Non-Invasive electrical and magnetic stimulation of the brain, spinal cord and roots: basic principles and procedures for routine clinical application. report of an IFCN committee. *Electroencephalogr. Clin. Neurophysiol.* 91, 79–92.

Rossini, P. M., Burke, D., Chen, R., Cohen, L. G., Daskalakis, Z., Di Iorio, R., et al. (2015). Non-Invasive electrical and magnetic stimulation of the brain, spinal cord, roots and peripheral nerves: basic principles and procedures for routine clinical and research application: an updated report from an I.F.C.N. Committee. *Clin. Neurophysiol.* 126, 1071–1107. doi: 10.1016/j.clinph.2015.02.001

Rosso, C., Perlbarg, V., Valabregue, R., Obadia, M., Kemlin-Méchin, C., Moulton, E., et al. (2017). Anatomical and functional correlates of cortical motor threshold of the dominant hand. *Brain Stimulation* 10, 952–958. doi: 10.1016/j.brs.2017.05.005

Rothwell, J. C., Hallett, M., Berardelli, A., Eisen, A., Rossini, P., and Paulus, W. (1999). Magnetic stimulation: motor evoked potentials. the international federation of clinical neurophysiology. *Electroencephalogr. Clin. Neurophysiol. Suppl.* 52, 97–103.

Schaworonkow, N., Triesch, J., Ziemann, U., and Zrenner, C. (2019). EEG-Triggered TMS reveals stronger brain state-dependent modulation of motor evoked potentials at weaker stimulation intensities. *Brain Stimulation* 12, 110–118. doi: 10.1016/j.brs.2018.09.009

Stokes, M. G., Chambers, C. D. I, Gould, C., Henderson, T. R., Janko, N. E., Allen, N. B., et al. (2005). Simple metric for scaling motor threshold based on scalp-cortex distance: application to studies using transcranial

magnetic stimulation. *J. Neurophysiol.* 94, 4520–4527. doi: 10.1152/jn.00067.2005

Tagliazucchi, E., von Wegner, F., Morzelewski, A., Brodbeck, V., and Laufs, H. (2012). Dynamic BOLD functional connectivity in humans and its electrophysiological correlates. *Front. Hum. Neurosci.* 6:339. doi: 10.3389/fnhum.2012.00339

Wassermann, E. M. (2002). Variation in the response to transcranial magnetic brain stimulation in the general population. *Clin. Nuerophysiol.* 113, 1165–1171.

Whitfield-Gabrieli, S., and Nieto-Castanon, A. (2012). Conn: a functional connectivity toolbox for correlated and anticorrelated brain networks. *Brain Connect.* 2, 125–141. doi: 10.1089/brain.2012.0073

Yaesoubi, M., Miller, R. L., and Calhoun, V. D. (2017). Time-varying spectral power of resting-state fmri networks reveal cross-frequency dependence in dynamic connectivity. *PLoS One* 12:e0171647. doi: 10.1371/journal.pone.0171647

Yushkevich, P. A., Piven, J., Hazlett, H. C., Smith, R. G., Ho, S., Gee, J. C., et al. (2006). User-Guided 3D active contour segmentation of anatomical structures: significantly improved efficiency and reliability. *NeuroImage* 31, 1116–1128. doi: 10.1016/j.neuroimage.2006.01.015

Ziemann, U., Lönnecker, S., Steinhoff, B. J., and Paulus, W. (1996). Effects of antiepileptic drugs on motor cortex excitability in humans: a transcranial magnetic stimulation study. *Ann. Neurol.* 40, 367–378. doi: 10.1002/ana.410400306

Zrenner, C., Desideri, D., Belardinelli, P., and Ziemann, U. (2018). Brain stimulation real-time EEG-de Fi ned excitability states determine Ef Fi Cacy of TMS-induced plasticity in human motor cortex. *Brain Stimulation* 11, 374–389. doi: 10.1016/j.brs.2017.11.016